PERGAMON

International Journal of Heat and Mass Transfer 42 (1999) 2199–2209

International Journal of HEAT and MASS TRANSFER

An experimental study of slot jet impingement cooling on concave surface: effects of nozzle configuration and curvature

Geunyoung Yang, Mansoo Choi*, Joon Sik Lee

Department of Mechanical Engineering, Seoul National University, Seoul 151-742, Korea

Received 20 March 1998; in final form 21 August 1998

Abstract

An experimental study has been carried out for jet impingement cooling on a semi-circular concave surface when jet flows were ejected from three different slot nozzles—round shaped nozzle, rectangular shaped nozzle and 2D contoured nozzle. Experiments have been conducted with variations of nozzle exit Reynolds number (Re_{2B}) in the range of $5920 \leqslant Re_{2B} \leqslant 25500$ and nozzle-to-surface distance (z_n) in the range of $1/2 \leqslant z_n/B \leqslant 20$ to determine the heat transfer coefficients under a constant heat flux condition. The developing structures of free jets were measured by hot-wire anemometer to understand the characteristics of heat transfer in conjunction with measured jet flows. Markedly different flow and heat transfer characteristics have been observed depending on different nozzle shapes. Average heat transfer rates for impingement on the concave surface are found to be more enhanced than the flat plate results due to the effect of curvature. Comparisons between the present results and the existing experimental results have also been made.

Nomenclature

A target surface area
B slot jet width
D inner diameter of circular concave surface
h convective heat transfer coefficient
I electrical current
k thermal conductivity
Nu_{2B} local Nusselt number
$Nu_{\mathrm{avg}(T_w)}$ average Nusselt number
$Nu_{2B,o}$ stagnation point Nusselt number
Re_{2B} nozzle exit Reynolds number
q_{loss} heat loss
q_g generated heat flux
q_w convective heat flux
s distance from the stagnation point along the cooled surface
T_j jet temperature
T_w wall temperature
u fluctuating velocity component
$\sqrt{u^2}$ RMS value of fluctuating velocity
U_{avg} average velocity in jet width direction at nozzle exit
U_j time-averaged mean velocity at the center of nozzle exit
U_m time-average local mean velocity
V voltage drop across the surface
x, y, z coordinates measured from nozzle center
z_n nozzle-to-target separation distance.

Greek symbols
υ kinematic viscosity
$\cos\phi$ power factor.

1. Introduction

Jet impingement cooling has been widely used to cool elements exposed to high temperature and high heat flux environments because of its advantages in the effective removal of locally concentrated heat and the easy adjustment to the location where the cooling is needed. Jet impingement techniques have been applied to many production processes including the drying of textiles, film and paper; the annealing of glass; the postprocessing of some metals and glass; the cooling of electronic equipment; and the freezing of tissue in cryosurgery. In particular, this jet impingement cooling has been effectively used

* Corresponding author

0017–9310/99/$ - see front matter
PII: S0017–9310(98)00337–8

to eliminate excessive thermal load near the leading edge of the inner surface of gas turbine blades and the outer wall of combustors.

Jet impingement cooling has been extensively studied for many years, and has been well recognized and reviewed. Empirical equations on jet impingement cooling for single round or slot nozzle and arrays of round or slot nozzles were provided for prediction of heat and mass transfer coefficients of many engineering applications [1]. Jambunathan et al. [2] reviewed previous data of single circular jet impingement cooling orthogonally onto a plane surface and clearly explained the significant effects of the nozzle geometry, the confinement of flow and the generation of turbulence from the jet nozzles on the jet impingement heat transfer. Heat transfer characteristics of single and multiple isothermal turbulent air jet impingement were also reviewed by Viskanta [3].

The impingement cooling has been studied mainly on a flat plate. When the impingement cooling is applied on a curved surface as in the jet impingement cooling onto the turbine blade inner surface, the curvature effect should be taken into consideration to understand the different phenomena between the flat plate case and the curved surface case. In general, for a flow on a surface with concave curvature, the centripetal force due to the curvature makes the flow unstable and a so-called Taylor–Görtler type vortex is produced [4, 5]. Such a vortex has its axis parallel to the flow direction and is known to enhance momentum and energy transfer and thereby heat transfer rate on the surface. However, the studies of jet impingement cooling on a curved surface are not encountered as frequently as those on a flat plate. Chupp et al. [6], Metzger et al. [7], and Tabakoff and Clevenger [8] measured impingement cooling on a semi-circled surface and investigated the effects of jet-to-jet spacing, the distance between the jet and the cooled surface, and various jet-hole arrangements. Dyban and Mazur [9] measured heat transfer coefficient on a parabolic concave surface and studied the effects of jet-flow passage curvature. Metzger et al. [10] and Bunker and Metzger [11] studied heat transfer characteristics for the different leading edge shapes of the cooled surface. Gau and Chung [12] visualized the jet flow impinging on both convex and concave semi-circular surfaces and showed the distinctive characteristics of flow and heat transfer on these surfaces. The nozzle configurations influence the jet impingement cooling efficiency significantly. Garimella and Nenaydykh [13] considered the effect of nozzle aspect ratios and diameters on flat plate cases. A wide variety of nozzles were tested to determine the effect of nozzle geometry on local convective heat transfer rate for jet impingement cooling on flat plate, and the heat transfer rate was changed depending on the jet flow structures developed from different nozzle conditions [14–16].

Most of the above studies of jet impingement cooling mainly focused on the heat and mass transfer characteristics, but the turbulent jet flow characteristics should be identified for a clear understanding of heat transfer phenomena and it is evident that the turbulent flow structure changes significantly depending on the nozzle shapes and thereby the heat transfer on the wall. Gardon and Akfirat [17, 18], Hoogendoorn [19], and Lytle and Webb [20] investigated the effect of turbulence on the heat transfer characteristics for jet impingement on flat plate. Therefore, it is important to specify jet flow conditions at nozzle exit in figuring out how the flow and the turbulence intensity vary for different nozzle shapes and how this flow structure affects the heat transfer characteristics. In this study, the effects of jet flows developed from three different slot nozzles (round shaped nozzle, rectangular shaped nozzle and 2D contoured nozzle) have been studied for the impingement heat transfer characteristics on a semi-circular concave surface. The present study is concerned with the effects of Reynolds number (Re_{2B}), curvature (concave surface case and flat plate case), and the spacing between the nozzle and the stagnation point on the target surface (z_n/B). The objective of the study is to explain the heat transfer characteristics of jet impingement cooling on a concave surface in relation to the turbulent jet-flow structure ejected from different shaped slot nozzles, and to figure out the curvature effect which may enhance the convective heat transfer rate.

2. Experimental apparatus and procedure

Figure 1 shows a schematic of the experimental apparatus for heat transfer measurement. The air was supplied from a blower and the total flow rate was controlled by an inverter. The heat exchanger was installed to obtain the constant temperature flow at the nozzle exit and to reduce the temperature difference between the ambient and the nozzle exit flow within $\pm 0.5^{\circ}$C. A uniform and stable flow distribution was established at the jet exit using a settling chamber of $400 \times 400 \times 600$ mm in volume and an acrylic duct 800 mm in length. To investigate the surface curvature effect, the semi-circular concave surface with 150 mm inner diameter and the flat plate were considered. The surface temperatures or the heat transfer coefficients along the cooled surface have been measured under a constant heat flux condition. In order to obtain the constant heat flux condition, high electric current was supplied through a thin stainless steel foil 30 μm in thickness. The generated heat flux (q_g) in the heating foil was controlled by the variation of output voltage, and calculated by measuring the voltage drop (V) between the voltage taps soldered in heating foil, the electrical current (I) and the power factor ($\cos\phi$). The thin stainless steel foil was bonded to the inner surface of the acrylic semi-circular surface by double-sided adhesive tape. Thermocouples were attached on the foil from an outer acrylic surface through drilled holes, and the void space

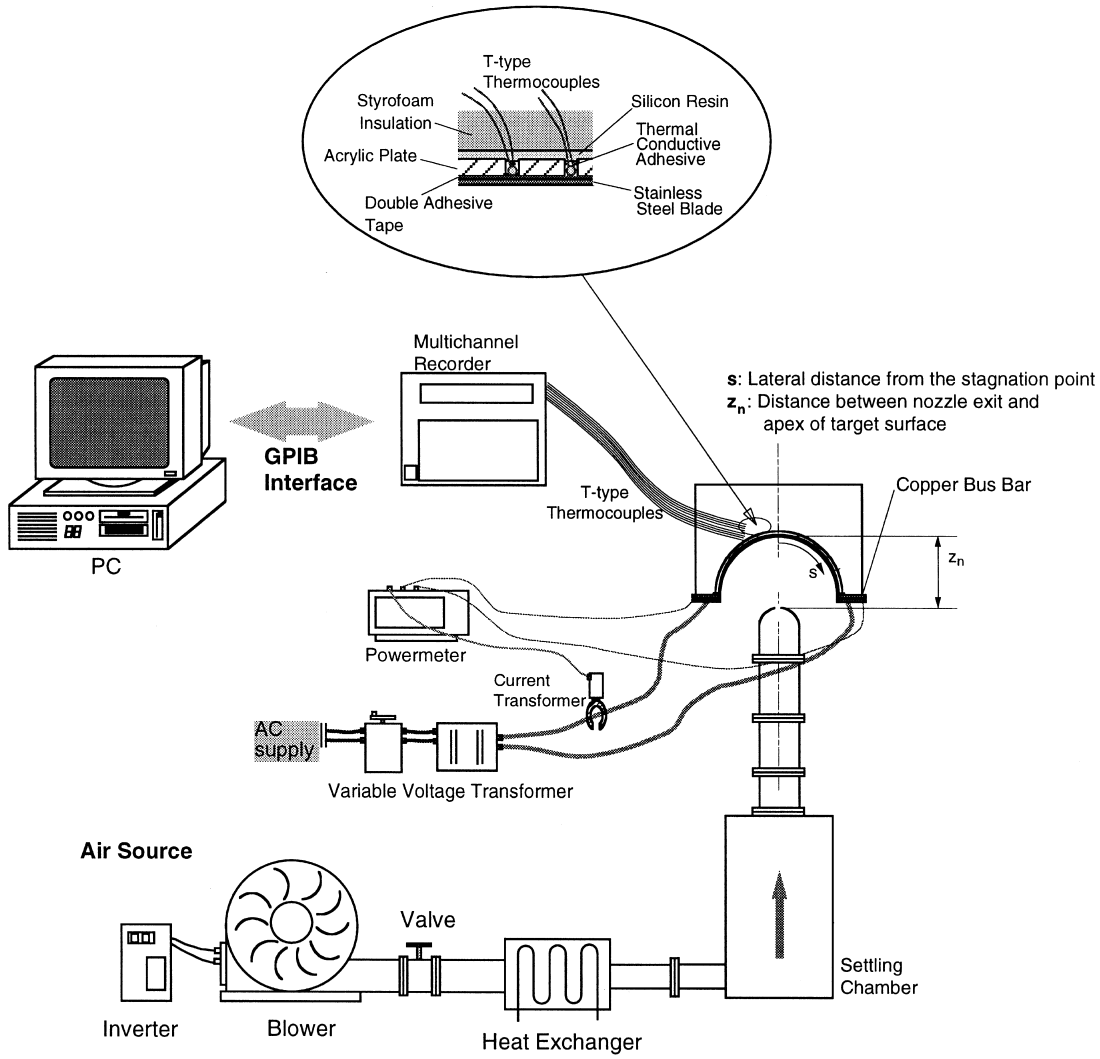

Fig. 1. Experimental apparatus for heat transfer measurements.

was completely filled with thermal epoxy. The outer acrylic surface was insulated with Styrofoam to reduce the conductive heat losses through the backward surface. To accomplish the negligible electrical contact resistance and the perfect contact between thin foil and bus bars, each end of heating thin foil was placed within two copper bus bars and bolted firmly. The wall temperature distribution (T_w), the ambient temperature (T_∞) and the jet temperature (T_j) were measured by T-type thermocouples 0.25 mm in diameter. Eighteen thermocouples were attached on the cooled surface along the flow direction from the stagnation point with an interval of 5 mm between each thermocouple to measure the wall temperature distribution, and the jet temperature was measured in the settling chamber to avoid the disturbance of the jet flow at the nozzle exit. The measured temperatures were recorded by a multi-channel recorder (Hybrid Recorder, YOKOKAWA) and stored in a personal computer through GPIB.

The experimental apparatus for flow measurements of jet flow and coordinate system is depicted in Fig. 2(a). Since jet impingement cooling efficiency is governed by forced convective heat transfer, the experiment of jet flow measurements was conducted separately without surface heating. The axial and spanwise variations of jet flow quantities ejected from three different nozzles were measured by hot-wire anemometer. The measured signals by using I-type hot-wire 5 μm in diameter (KANOMAX) and CTA module (56C01, DANTEC) were filtered and amplified in a signal processor (56N20, DANTEC) at 30 kHz cutoff frequency, then the output analog signals were converted and recorded at the personal computer

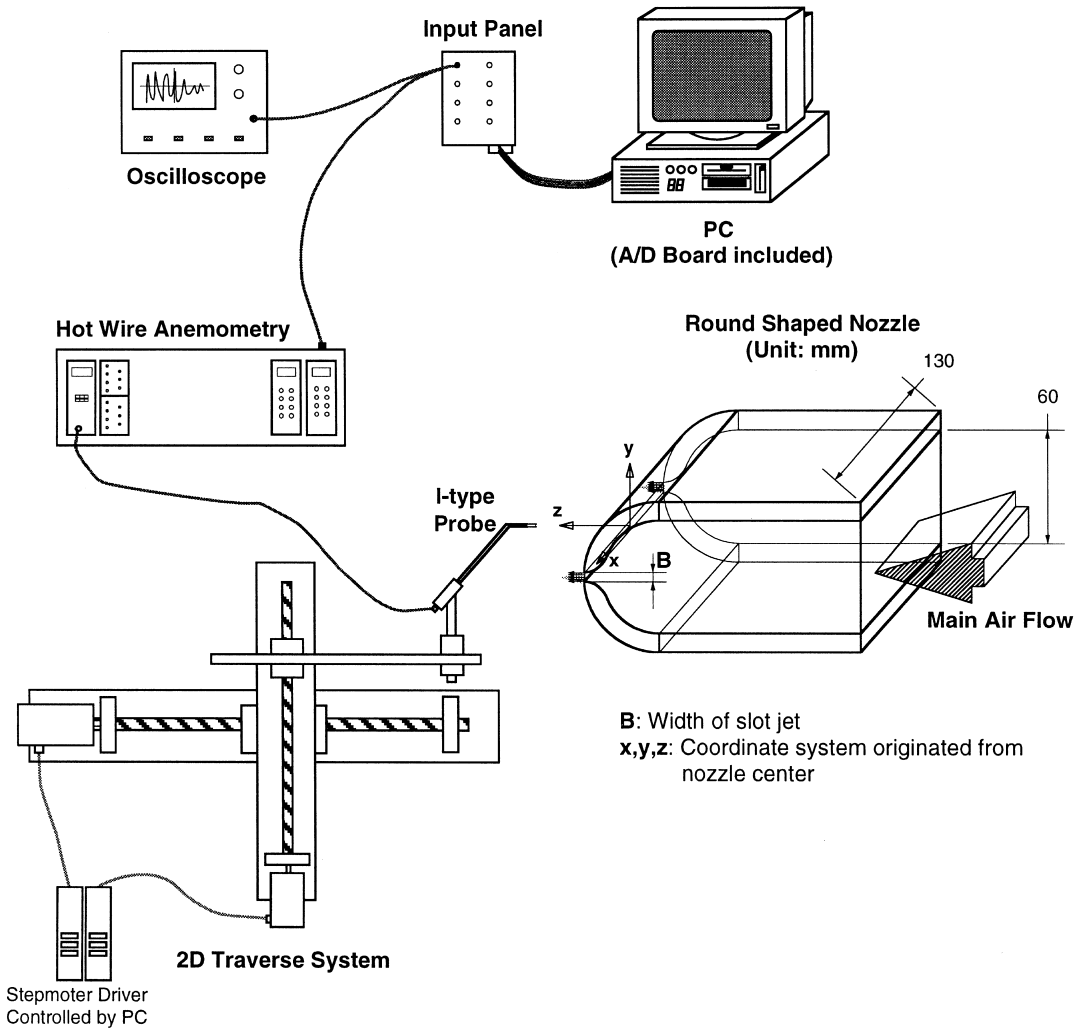

(a) Schematic of flow measurement

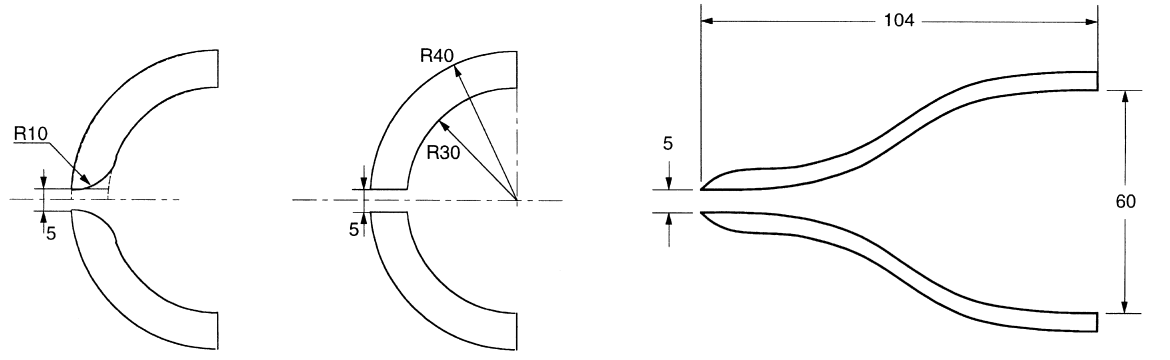

(b) Nozzle geometry

Fig. 2. Experimental apparatus for flow measurements and nozzle geometry: (a) schematic of flow measurement; (b) nozzle geometry.

including the A/D board (DT2838, Data Translation) with 16 bit resolution. To obtain mean velocity and turbulence intensity of jet flow, the hot-wire signals were sampled at 20 kHz and 600 000 acquisition data at a measuring position were converted to instantaneous velocities by using the correlation curve based on King's law. To evaluate the turbulence intensity of jet flow, the RMS value of velocity fluctuation ($\sqrt{u^2}$) is normalized by the jet velocity (U_j) at the nozzle exit center instead of local mean velocity (U_m), and this normalized value indicates the absolute magnitude of velocity fluctuation at the measuring point [17, 20]. A two-axes traversing device with stepping motors controlled through a digital output from an I/O board in a personal computer enables a hot-wire probe and a pitot tube to be located at the right measuring point within 15 μm spatial resolution.

To take account of the distinctive behavior of flow and heat transfer, particularly of flow turbulence for different nozzle shapes, three nozzles of 5 mm in slot width were considered (shown in Fig. 2(b)). The round shaped nozzle and the rectangular shaped nozzle were made by cutting an acrylic tube 60 mm inner diameter and 80 mm outer diameter. The inlet of the round shaped nozzle was rounded with a radius of curvature of 10 mm, and the exit of the rectangular shaped nozzles was made into a rectangular channel with aspect ratio equal to 2. The 2D contoured nozzle was designed according to the method suggested by Morel [21] for the 2D contraction part of a wind tunnel.

When the jet flow ejected from three different slot nozzles impinges on the semi-circular concave surface and flat plate under a constant heat flux condition, wall temperatures have been measured with variations of nozzle exit Reynolds number (Re_{2B}) in the range of $5920 \leqslant Re_{2B} \leqslant 25500$ and the nozzle-to-surface distance (z_n) in the range of $1/2 \leqslant z_n/B \leqslant 20$ to determine the heat transfer coefficients. About 1 h was required for the achievement of thermal steady condition after the startup of wall heating.

Mean velocities have been evaluated from the difference between total and static pressures of pitot tube along the spanwise direction to calculate the average velocity (U_{avg}) over the slot width at the nozzle exit. The Reynolds and Nusselt numbers were calculated on the basis of the hydraulic diameter for slot nozzle, $2B$, properties at jet temperature and measured data.

$$Re_{2B} = \frac{U_{avg} \cdot 2B}{\upsilon} \tag{1}$$

$$Nu_{2B} = \frac{h \cdot 2B}{k} = \frac{q_w}{T_w - T_j}\frac{2B}{k} \tag{2}$$

The minimum temperature difference ($T_w - T_j$) between the wall temperature and jet temperature has been made larger than 15°C to minimize the effect of temperature measurement errors. The convective heat flux (q_w) was calculated as follows:

$$q_w = q_g - q_{loss} \approx \frac{VI\cos\phi}{A} \tag{3}$$

When the heat flux is determined, several heat losses have been estimated. The conduction heat losses through insulation material, through thermocouple wires and from the side edge of the stainless steel foil were estimated to be less than 0.5, 0.1 and 0.02% of the total generation of heat in the foil, respectively, because of the 30 μm thickness of the foil and small conductivity of insulating material (Styrofoam: $k = 0.03$ W m^{-1} K^{-1}). The heat loss due to radiation was estimated by using the emissivity of stainless steel foil ($\varepsilon = 0.17$) and view factor value of one, and was found to be less than 1.8% because of low wall temperatures.

The uncertainty analysis was performed for the measurement values by using methods suggested by Kline and McClintock [22] with 95% confidence level. For given conditions ($U_j = 40$ m s^{-1}, $z_n/B = 1/2$ for a round shaped nozzle) the relative uncertainties of heat flux and heat transfer coefficient are 1.6 and 5.4%, respectively. The overall relative uncertainty in the Nusselt number is estimated as 6.4% and the relative uncertainty in the Reynolds number is estimated to be 3.8%.

3. Results and discussion

To characterize three nozzles used, spanwise distributions of mean velocities (Fig. 3) and velocity fluctuations (Fig. 4) of free jets have been measured for different axial distances from the nozzle exit in the range of $0.2 \leqslant z/B \leqslant 12$ when center velocity at the nozzle exit, U_j, was equal to 40 m s^{-1}. The distributions of normalized mean velocity in the spanwise direction for the round shaped nozzle (Fig. 3(a)) and the rectangular shaped nozzle (Fig. 3(b)) show markedly different jet flow characteristics. For round shaped nozzle results, mean velocity at $z/B = 0.2$ is almost equal to the nozzle exit velocity throughout the nozzle width. It is shown that the shear flow region developed from the edge of the nozzle is expanding due to the mixing of jet flow and ambient air, and beyond $z/B = 6$ the effect of entrainment penetrates up to the center line. When the jet flow develops to the downstream with the increase of axial distance (z/B), ambient flows are entrained up to the potential core region of a jet flow and the uniform distribution of velocity that occurred at the nozzle exit becomes the bell-shaped distribution. The overall trend is similar irrespective of nozzle exit velocities. For the rectangular shaped nozzle case, the region with uniform velocities along the jet width does not appear, and the rectangular shaped nozzle yields less flat velocities and a faster reduction of the center velocity than the round shaped nozzle. This would be due to the pre-development of jet flow along the rectangular shaped flow passage. Because

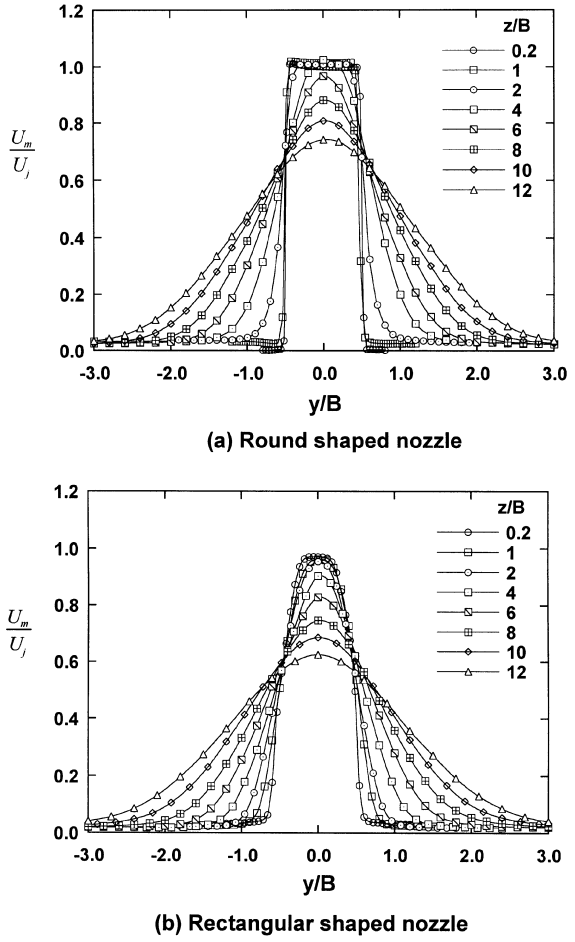

Fig. 3. Widthwise variations of mean velocity for different nozzle shapes at $U_j = 40\ \mathrm{m\ s^{-1}}$: (a) round shaped nozzle; (b) rectangular shaped nozzle.

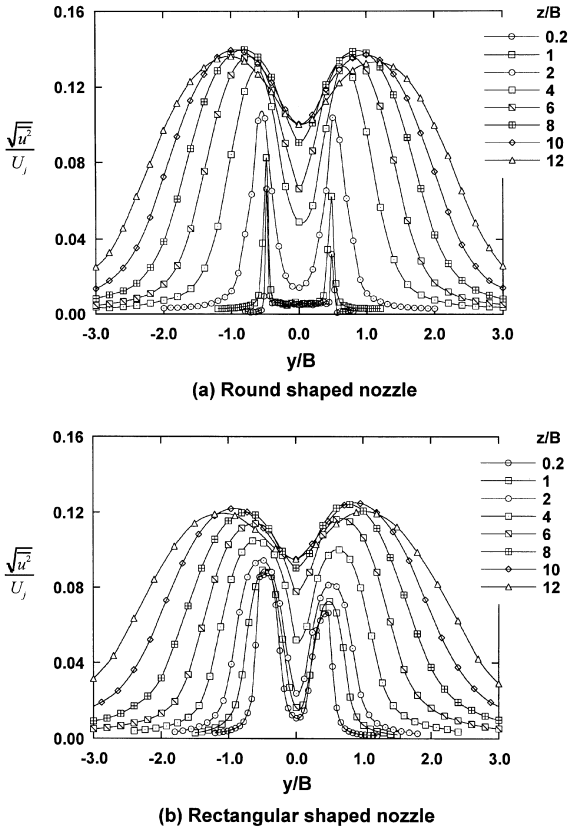

Fig. 4. Widthwise variations of velocity fluctuations for different nozzle shaped at $U_j = 40\ \mathrm{m\ s^{-1}}$: (a) round shaped nozzle; (b) rectangular shaped nozzle.

of non-uniform velocity at the nozzle exit, the shear layer grows earlier than for the case of a round shaped nozzle and the vigorous entrainment of ambient flow is expected. The jet velocity structure of 2D contoured nozzle is similar to the round shaped nozzle results due to the similarity of the edge shape at the nozzle exit.

Figure 4 shows the normalized velocity fluctuations, i.e. turbulence intensities, in the widthwise direction for a round shaped nozzle and a rectangular shaped nozzle at $U_j = 40\ \mathrm{m\ s^{-1}}$. For the round shaped nozzle (Fig. 4(a)), the region with uniform and low turbulence intensities exists near the nozzle exit. Turbulence intensity grows sharply near the nozzle edge, $y/B = \pm 0.5$, due to the mixing in the shear layers where large velocity gradients exist. Since the mixing layer expands as the axial distance increases, the location where the maximum turbulence intensity occurs becomes farther from the nozzle centerline with the increase of z/B. At $z/B = 8$ the maximum turbulence intensity is about 14% near $y/B = \pm 0.8$, and in the downstream region the maximum turbulence intensity in the spanwise direction decreases. Turbulence intensities at the jet centerline increase with the increase of z/B until $z/B \leqslant 10$. Turbulence intensity at the exit of the rectangular shaped nozzle is not uniform along the jet width, and larger than that for the round shaped nozzle, which is resulted from the different flow passage within the nozzle. A jet flow ejected from the rectangular shaped nozzle can be developed to some extent while flowing in a rectangular shaped flow passage, and the widthwise distribution of jet flow at the nozzle exit is similar to that obtainable from a developing channel flow. It is emphasized that the flow development along the flow passage resulted in less flat velocities at the exit of a rectangular shaped nozzle (see Fig. 3(b)). Although the centerline turbulence intensities for a rectangular shaped nozzle are a little larger than those for a round shaped nozzle, the maximum turbulence intensity which occurs off the centerline is smaller because of smaller velocity gradient near the shear layer; the maximum tur-

bulence intensity for the rectangular shaped nozzle is about 12% at $z/B = 8$.

The different developing structure of jet flows which depend on nozzle shapes can be seen from the distributions of mean velocity and turbulence intensity along the centerline (Fig. 5). Figure 5 shows the axial variations of jet flows along the centerline for three different nozzles with the increase of axial distance from nozzle exit in the range of at $0 \leqslant z/B \leqslant 20$ at $U_j = 10$ and 40 m s^{-1}. Mean velocities at the nozzle exit maintain for some distances within the potential core region, then decrease in different ways depending on nozzle shapes. Potential core length for a round shaped nozzle is longer than those for two other nozzles, and the rectangular shaped nozzle results in the shortest potential core length. The round shaped nozzle and 2D contoured nozzle can carry fluids in the centerline to the farther downstream region with a little loss of momentum by preventing the penetration of shear effect into the jet centerline due to the uniform velocity along the jet width at the nozzle exit (see Fig. 3(a)). Turbulence intensities for round shaped and 2D contoured nozzles maintain nozzle exit value up to z equal to $2B$, and increase sharply before reaching the maximum value that occurs near $8B \sim 10B$. However, the rectangular shaped nozzle shows the increase of turbulence intensity from the nozzle exit without the region of constant turbulence intensity, which can be inferred from the fact of the flow pre-development through the flow passage. The maximum turbulence intensity for the round shaped nozzle is about 17% at $U_j = 10$ m s^{-1} and 11% at $U_j = 40$m s^{-1}, respectively. Near the nozzle exit, the rectangular shaped nozzle results in larger turbulence intensity than round shaped and 2D contoured nozzles because of the pre-development of a jet flow.

These different jet flow structures for different nozzle shapes should influence the impinging jet flow structure, and finally the heat transfer characteristics. Figure 6 shows the stagnation point and average Nusselt numbers for different nozzles and jet Reynolds numbers with the

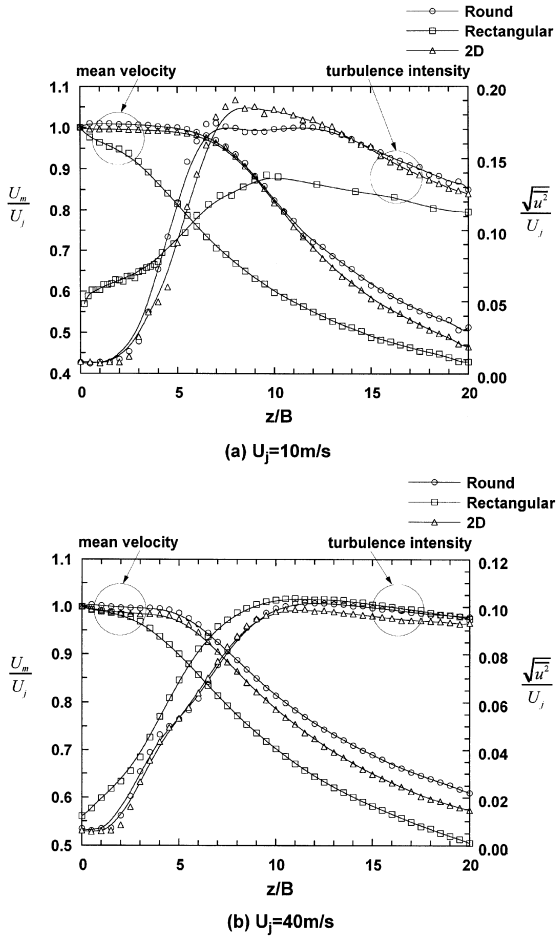

Fig. 5. Axial variations of jet flow structure for different nozzle shapes: (a) $U_j = 10$ m s^{-1}; (b) $U_j = 40$ m s^{-1}.

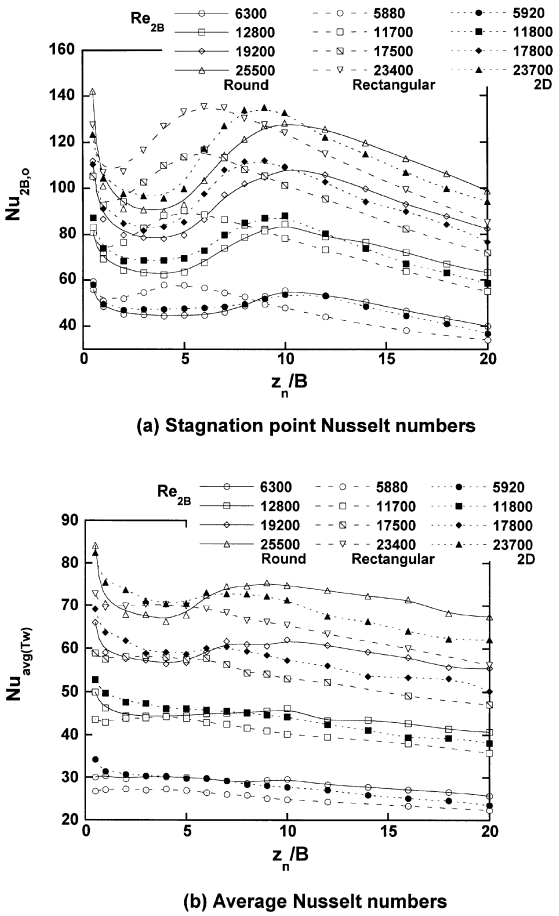

Fig. 6. Heat transfer results for different nozzle shapes: (a) stagnation point Nusselt numbers; (b) average Nusselt numbers.

increase of nozzle-to-surface distance in the range of $1/2 \leqslant z_n/B \leqslant 20$. For the case of the round shaped nozzle, the stagnation point Nusselt number is the highest at the smallest spacing, $z_n/B = 1/2$ and decreases as the distance between the nozzle exit and target surface (z_n/B) is increased. From z_n/B equal to approximately 2–4, the Nusselt number again increases up to a peak occurred near $z_n/B = 10$. This spacing where a peak occurs, approximately coincides with the location of the maximum turbulence intensity at the centerline (see Fig. 5). Within this region ($z_n/B \leqslant 10$) mean velocities do not vary significantly, but the magnitude of velocity fluctuations increases substantially, which causes the heat transfer rate to increase. For the case of a rectangular shaped nozzle, a similar trend has been observed. However, a peak Nusselt number occurs at the smaller spacing; $z_n/B = 4$–6 compared to the case of a round shaped nozzle because the decay of centerline velocity commences at shorter distance from the nozzle exit (see Fig. 5). Different flow characteristics obviously resulted in different heat transfer behavior and can explain why the peak of heat transfer rate occurred at the spacing of $z_n/B \approx 10$ for a round shaped nozzle and $z_n/B = 4$–6 for a rectangular shaped nozzle, respectively. For large spacings, the stagnation point Nusselt number for a round shaped nozzle becomes larger than those for 2D contoured and rectangular shaped nozzles, which can be inferred from the fact that mean velocity for the round shaped nozzle is larger in the free jet downstream region than the case of other two nozzles (see Fig. 5). For all nozzles considered, the highest heat transfer rates at the stagnation point occur at the smallest spacing, at $z_n/B = 1/2$. This seems to be due to the effect of fluid acceleration between the nozzle exit and impingement surface [20]. Gardon and Akfirat [17] reported that the boundary layer thickness near the stagnation region in which the velocity varies from free jet condition to zero on the surface was approximately equal to 1.1–1.2 nozzle diameter for a single round jet. The boundary layer thickness in the stagnation region for a slot jet impingement varies depending on the nozzle-to-surface distances and nozzle exit velocities [23]. The small spacings, $z_n/B \leqslant 3$ for round shaped and 2D contoured nozzle, seem to be within the boundary layer for the stagnation region. Therefore, smaller spacings can cause larger axial velocity gradients and also larger temperature gradients on the surface than cases with $z_n/B > 3$, which enhances the heat transfer rate. For average Nusselt numbers based on mean wall temperature (Fig. 6(b)), the average heat transfer rate of 2D contoured nozzle is better than other two nozzles at small z_n/B. As z_n/B increase, average Nusselt numbers for round shaped nozzle become larger due to larger mean velocities than those for other two nozzles. The average Nusselt number for the 2D contoured nozzle is more uniform in the broad range of z_n/B. From the view point of stagnation point Nusselt number, shorter spacings from the nozzle exit to the impinging surface seem to be necessary if the rectangular shaped nozzle is used, while larger spacing would be desirable for round shaped and 2D contoured nozzles if very small spacings are avoided.

The variations of local Nusselt numbers for three nozzles along the concave surface from the stagnation point have been compared with the results reported by Gau and Chung [12] in Fig. 7. The present results for all nozzles considered show similar trend to Gau and Chung [12] for $z_n/B = 12$, however, for $z_n/B = 4$ (Fig. 7(a)), rectangular shaped nozzle results in much different Nusselt numbers from the other cases. The higher Nusselt number at the stagnation point ($s/B = 0$ case in Fig. 7(a)) for a rectangular shaped nozzle would be inferred from higher turbulence intensity along the jet centerline for a free jet (shown in Fig. 5(b)). However, higher Nusselt number observed up to the circumferential distance s/B equal to about 6 for a rectangular shaped nozzle can not be

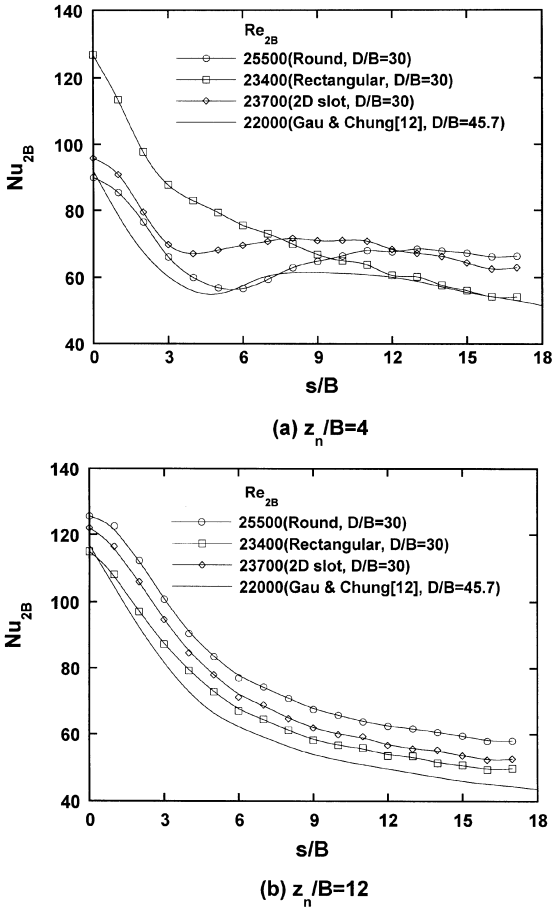

Fig. 7. Comparison of local Nusselt numbers with Gau and Jung [12] results for different nozzle shapes: (a) $z_n/B = 4$; (b) $z_n/B = 12$.

explained from the free jet measurements alone, but the additional data for the distribution of developing wall jet should be measured for a proper explanation (this has not been done in the present study). Even though free jet turbulence intensity distribution in the jet widthwise direction for a rectangular shaped nozzle seems to show smaller values as a whole than for a round shaped nozzle, the distribution of wall jet flow turbulence can produce different trends since the wall jet has been developed from the stagnation point where the rectangular shaped nozzle shows higher turbulence intensity of a free jet. The secondary peaks have been observed at small spacings such as $z_n/B = 4$ shown in Fig. 7(a) except for the rectangular shaped nozzle, while peaks did not occur for large spacings of $z_n/B = 12$. The existence of secondary peaks has been thought to be due to the transition of the stagnation flow from a laminar wall jet flow to a turbulent wall jet flow [17, 20]. The fact that the rectangular shaped nozzle produced sufficiently large turbulence of a free jet at $z_n/B = 4$ (shown in Fig. 5) would suggest that a notable increase of turbulence intensity along the curved surface may not occur, correspondingly, heat transfer rates may decrease monotonously along the surface without a secondary peak. Gardon and Akfirat [17] also reported that the secondary peak disappeared for the impinging jet with artificially induced turbulence at the nozzle exit. To figure out the effect of jet exit velocity on the secondary peak phenomena of heat transfer rate along the streamwise direction, the local Nusselt numbers for the round shaped nozzle are plotted in Fig. 8 for different jet Reynolds numbers in the range of at $6300 \leqslant Re_{2B} \leqslant 25500$ at $z_n/B = 1/2$. As the Reynolds number increases, the secondary peak of local Nusselt number occurs more prominently and the location where the secondary peak occurs moves toward the stagnation point because of the earlier occurrence of transition for higher jet Reynolds numbers.

Figure 9 shows the comparisons of heat transfer rates for impingement on the semi-circular concave surface ($D/B = 30$) and the flat plate; Fig. 9(a): stagnation point Nusselt numbers; Fig. 9(b): average Nusselt numbers. The heat transfer rates at the stagnation point are almost similar for two cases, however, the average heat transfer rates are different and this trend becomes more prominent for higher Reynolds numbers. While the stagnation region is not affected seriously by the surface curvature, the instabilities such as Taylor–Görtler vortex induced by the concave curvature would grow along the streamwise direction and enhance the heat transfer rates further in the downstream region apart from the stagnation point. Correspondingly, the average Nusselt numbers should be more influenced by curvature than the stagnation point

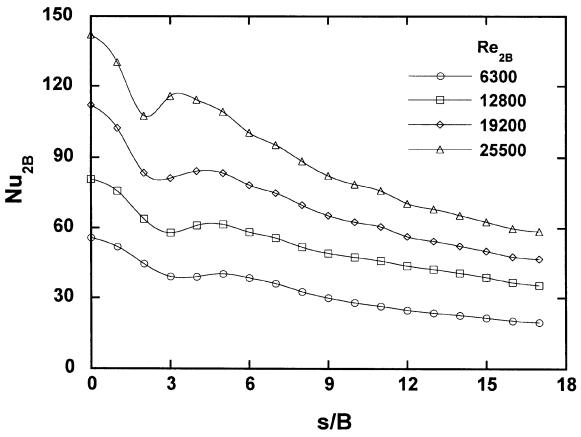

Fig. 8. Variations of secondary peak of local Nusselt numbers with increasing Reynolds number for round shaped nozzle at $z_n/B = 1/2$.

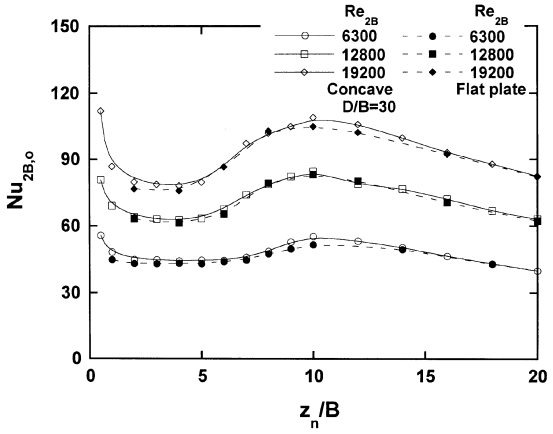

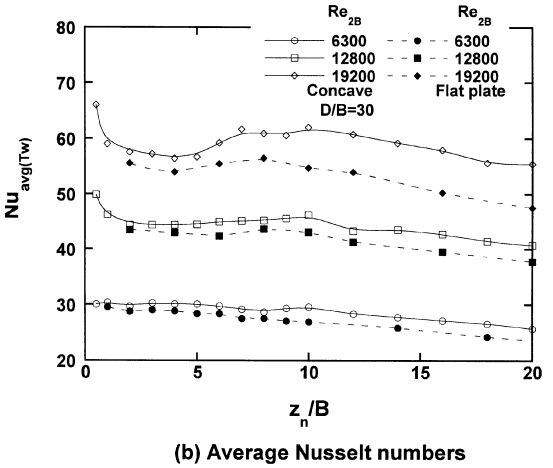

Fig. 9. Comparison of Nusselt numbers on concave surface and on flat plate for round shaped nozzle: (a) stagnation point Nusselt numbers; (b) average Nusselt numbers.

Nusselt numbers and are shown to become larger than flat plate results.

4. Conclusions

Jet impingement cooling on the concave surface has been studied for three different nozzle configurations. The effects of nozzle shapes, the curvature, Reynolds numbers and the spacings between the nozzle exit and cooled surface are of primary interests. The following conclusions have been drawn.

(1) Markedly different flow characteristics have been observed when different nozzles were used, and heat transfer characteristics were also significantly different for different nozzles and have been successfully explained in conjunction with the measured flow characteristics.
(2) As the spacing between the nozzle exit and the cooled concave surface was increased, there was a region where the stagnation point Nusselt number increased before reaching a peak. This phenomenon results from the increase of turbulence intensity of jet flow within the potential core region. The spacing where a peak stagnation point Nusselt number occurs corresponds approximately to the location of the maximum turbulence intensity of a free jet for round shaped and 2D contoured nozzles. Since the jet flow issued from the rectangular shaped nozzle is developed earlier and the turbulence intensity increases sharply when the jet flow passes through the sharp nozzle edge, the rectangular shaped nozzle results in an earlier increase of stagnation point Nusselt number as the spacing is increased.
(3) Secondary peaks have been observed for small spacings between nozzle exit and concave surface. As jet Reynolds number increases, the secondary peak occurs more prominently and the location where the secondary peak occurs moves toward the stagnation point because of the earlier occurrence of transition for higher Reynolds numbers.
(4) The effect of curvature has been studied by comparing with flat plate results and is shown to be significant. For $D/B = 30$, the average heat transfer rates were enhanced even though the heat transfer rates at the stagnation point for concave surface were almost same as those on flat surface. The effect of curvature becomes more prominent as Reynolds number increases.

Acknowledgements

This work was supported by Turbo and Power Machinery Research Center, Korea Science and Engineering Foundation.

References

[1] H. Martin, Heat and mass transfer between impinging gas jets and solid surface, Advances in Heat Transfer 13 (1977) 1–60.
[2] K. Jambunathan, E. Lai, M.A. Moss, B.L. Button, A review of heat transfer data for single circular jet impingement, International Journal of Heat and Fluid Flow 13 (1992) 106–115.
[3] R. Viskanta, Heat transfer to impinging isothermal gas and flame jets, Experimental Thermal and Fluid Science 6 (1993) 111–134.
[4] H. Thomann, Effect of streamwise wall curvature on heat transfer in a turbulent boundary layer, Journal of Fluid Mechanics 33 (1968) 283–292.
[5] R.E. Mayle, M.F. Blair, F.C. Kopper, Turbulent boundary layer heat transfer on curved surfaces, Journal of Heat Transfer 101 (1981) 521–525.
[6] R.E. Chupp, H.E. Helms, P.W. McFadden, T.R. Brown, Evaluation of internal heat transfer coefficients for impingement-cooled turbine airfoils, Journal of Aircraft 6 (1969) 203–208.
[7] D.E. Metzger, T. Yamashita, C.W. Jenkins, Impingement cooling of concave surfaces with lines of circular air jets, Journal of Engineering for Power 91 (1969) 149–158.
[8] W. Tabakoff, W. Clevenger, Gas turbine blade heat transfer augmentation by impingement of air jets having various configurations, Journal of Engineering for Power 94 (1972) 51–60.
[9] Y.P. Dyban, A.I. Mazur, Heat transfer from a flat air jet flowing into a concave surface, Heat Transfer—Soviet Research 2 (1970) 15–20.
[10] D.E. Metzger, R.T. Baltzer, C.W. Jenkins, Impingement cooling performance in gas turbine airfoils including effects of leading edge sharpness, Journal of Engineering for Power 94 (1972) 219–225.
[11] R.S. Bunker, D.E. Metzger, Local heat transfer in internally cooled turbine airfoil leading edge regions, part I—impingement cooling without film coolant extraction, Journal of Turbomachinery, 112 (1990) 451–458.
[12] C. Gau, C.M. Chung, Surface curvature effect on slot air-jet impingement cooling flow and heat transfer process, Journal of Heat Transfer 113 (1991) 858–864.
[13] S.V. Garimella, B. Nenaydykh, Nozzle-geometry effects in liquid jet impingement heat transfer, International Journal of Heat and Mass Transfer 39 (1996) 2915–2923.
[14] D.W. Colucci, R. Viskanta, Effect of nozzle geometry on local convective heat transfer to a confined impinging air jet, Experimental Thermal and Heat Fluid Science 13 (1996) 71–80.
[15] M. Gundappa, J.F. Hudson, T.E. Diller, Jet impingement heat transfer from jet tubes and orifices, Proceedings of National Heat Transfer Conference, HTD vol. 107, 1989, pp. 43–50.
[16] C.O. Popiel, L. Boguslawski, Mass or heat transfer in impinging single, round jets emitted by a bell-shaped nozzle and sharp-ended orifice, Proceedings of the Eighth International Heat Transfer Conference, vol. 3, 1986, pp. 1187–1192.
[17] R. Gardon, J.C. Akfirat, The role of turbulence in deter-

mining the heat-transfer characteristics of impinging jets, International Journal of Heat and Mass Transfer 8 (1965) 1261–1272.
[18] R. Gardon, J.C. Akfirat, Heat transfer characteristics of impinging two-dimensional air jets, Journal of Heat Transfer 88 (1966) 101–108.
[19] C.J. Hoogendoorn, The effect of turbulence on heat transfer at a stagnation point, International Journal of Heat and Mass Transfer 20 (1977) 1333–1338.
[20] D. Lytle, B.W. Webb, Air jet impingement heat transfer at low nozzle-plate spacings, International Journal of Heat and Mass Transfer 37 (1994) 1687–1697.
[21] T. Morel, Design of two-dimensional wind tunnel contractions, Journal of Fluids Engineering 99 (1977) 371–377.
[22] S.J. Kline, F.A. McClintock, Describing uncertainties in single-sample experiments, Mechanical Engineering 75 (1953) 3–8.
[23] H.S. Yoo, An experimental study on heat transfer and fluid flow in jet impingement cooling of concave surface, M.S. thesis, Seoul National University, Korea, 1995.